DOI: 10.1002/chem.200800806

Zipped-Up Chain-Type Coordination Polymers: Unsymmetrical Amide-Containing Ligands Inducing β-Sheet or Helical Structures

Kazuhiro Uemura,*[a] Yuki Kumamoto,[b] and Susumu Kitagawa[b, c, d]

Abstract: The crystal structures of thirteen Ag^I coordination polymers involving py-CONH-$(CH_2)_n$-py (py = pyridine; $n = 0$, 1) derivatives were determined by means of single-crystal X-ray analyses. All of the compounds form one-dimensional chains composed of Ag^I atoms and bridging ligands with formulas $\{[Ag(py\text{-}CONH\text{-}(CH_2)_n\text{-}py)][X]\}_n$ ($X = PF_6^-$, ClO_4^-, BF_4^-, and NO_3^- with solvent molecules). The unsymmetrical coordination environments around Ag^I atoms induce direction in the chains, that is, -[NH-$(CH_2)_n$-py-Ag-py-CO]-, which resembles the alignment of amino acid chains in proteins. In compounds $\{[Ag(4\text{-}pia)][X]\}_n$ (**1**⊃X; 4-pia = *N*-(4-pyridyl)isonicotinamide; $X = PF_6^-$, ClO_4^-, BF_4^-, and NO_3^-), $\{[Ag(4\text{-}pmia)][X]\}_n$ (**2**⊃X; 4-pmia = *N*-(pyridin-4-ylmethyl)isonicotinamide; $X = PF_6^-$, $ClO_4^-\cdot H_2O$, and $NO_3^-\cdot H_2O$), and $\{[Ag(3\text{-}pmia)][X]\}_n$ (**3**⊃X; 3-pmia = *N*-(pyridin-3-ylmethyl)isonicotinamide; $X = PF_6^-$, ClO_4^-, BF_4^-, and $NO_3^-\cdot H_2O$), each chain is aligned parallel to neighboring chains, but adjacent chains run in the opposite direction. Particularly in $\{[Ag(3\text{-}pmia)][PF_6]\}_n$ (**3**⊃PF_6^-), $\{[Ag(3\text{-}pmia)][ClO_4]\}_n$ (**3**⊃ClO_4^-), and $\{[Ag(3\text{-}pmia)][BF_4]\}_n$ (**3**⊃BF_4^-), amide moieties of 3-pmia ligands are complementarily hydrogen bonded to amide moieties in neighboring chains, as in the β-sheet motif in proteins. On the other hand, in $\{[Ag(4\text{-}pmna)][PF_6]\cdot MeOH\}_n$ (4-pmna = *N*-(pyridin-4-ylmethyl)nicotinamide), all chains in the crystal form left-handed (**4a**⊃$PF_6^-\cdot$MeOH) and right-handed (**4b**⊃$PF_6^-\cdot$MeOH) helical structures with a helical pitch of 28 Å. Heterogeneous anion exchanges proceed reversibly in **2**, but not in **3**, which provides information about the thermal stabilities of the crystals.

Keywords: amides · coordination polymers · hydrogen bonds · silver

Introduction

Crystal engineering by exploiting noncovalent forces has attracted much attention in recent years due to the challenge of constructing novel solid architectures,[1–3] particularly porous coordination polymers.[1] This field of research has been developed and accelerated by means of simple strategies, such as the hydrogen-bonded supramolecular synthon[2c] and the use of secondary building units (SBUs),[1d] which provide effective guidelines for constructing derivative architectures. In particular, supramolecular synthons describe the precise recognition events that take place when molecules assemble, a concept that has prompted numerous reports about the crystal structures of hydrogen-bonded organic molecules.[2,3] Furthermore, the idea of combining coordination polymers and ligand-based hydrogen bonds has been introduced recently,[2e] opening up a new dimension in this field.

There are some advantages to this approach because it allows a combination of strength, imparted by a coordination network, and flexibility, allowed by the softer hydrogen-bonding interactions.[4] In fabricating networks using both noncovalent forces, the design of organic ligands is important because hydrogen-bonding sites can possibly coordinate to metals, resulting in unpredicted crystal structures. Despite these inherent difficulties, the following organic li-

[a] Dr. K. Uemura
Environmental Science and Engineering
Graduate School of Science and Engineering, Yamaguchi University
Tokiwadai 2-16-1, Ube-shi, Yamaguchi 755-8611 (Japan)
Fax: (+81) 836-85-9601
E-mail: kazu-u@yamaguchi-u.ac.jp

[b] Y. Kumamoto, Prof. Dr. S. Kitagawa
Department of Synthetic Chemistry and Biological Chemistry
Graduate School of Engineering, Kyoto University
Katsura, Nishigyo-ku, Kyoto 615-8510 (Japan)

[c] Prof. Dr. S. Kitagawa
Institute for Integrated Cell-Material Sciences (iCeMS)
Kyoto University, 69 Konoe-cho
Yoshida, Sakyo-ku, Kyoto 606-8501 (Japan)

[d] Prof. Dr. S. Kitagawa
ERATO Kitagawa Integrated Pore Project, Kyoto Research Park
Bldg #3, Shimogyo-ku, Kyoto, 600-8813 (Japan)

Supporting information for this article is available on the WWW under http://dx.doi.org/10.1002/chem.200800806.

gands combined with metals have afforded rationally built-up structures: py-amide (py = pyridine),[5] py-urea-py,[6] py-amide-py,[7,8] and py-(amide)$_2$-py types[6a,9] (Scheme 1). In

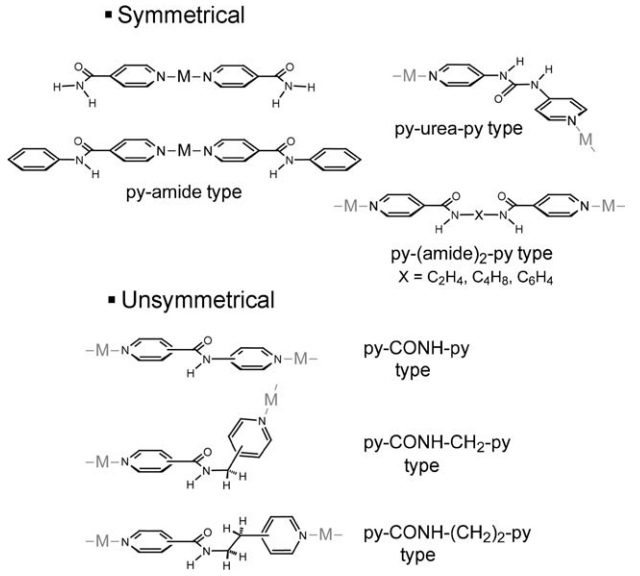

Scheme 1. Different types of symmetrical and unsymmetrical organic ligands that can be used to construct crystal structures when combined with metals.

the crystal structures constructed by using these organic ligands, pyridine moieties are coordinated to metal ions, whereas amide and urea moieties interact through hydrogen bonds, to avoid the coordination of hydrogen-bonding sites to metals, thus raising the possibility of dealing rationally with both coordination and hydrogen bonds. Furthermore, by using coordination polymers instead of discrete molecular assemblies, the resulting structures have fewer degrees of freedom, thereby facilitating structural prediction and control.

On this basis, we have prepared the unsymmetrical amide-containing ligands, py-CONH-py, py-CONH-CH_2-py, and py-CONH-$(CH_2)_2$-py, in which two pyridyl groups are bridged by -CONH-, -CONH-CH_2-, and -CONH-$(CH_2)_2$- moieties, respectively (Scheme 1), to add a new structural dimension to coordination networks having a β-sheet motif[10] by incorporating cross-linked coordination-based motifs. The backbone of these ligands is an amide moiety, which is well known for its typical hydrogen-bonding network. Coordination polymers derived from these ligands are expected to self-assemble through complementary hydrogen bonds involving an amide backbone. Previously, we have reported the synthesis and structures of square grids[8a,b] and repeated rhomboid-type chains[8c] with these types of ligands. Especially in square grids $[Co(X)_2(3\text{-pna})_2]_n$ (3-pna = *N*-(pyridin-3-yl)nicotinamide; $X = NCS^-$, NO_3^-, and Br^-) and $\{[Co(NCS)_2(4\text{-peia})_2]\cdot 4Me_2CO\}_n$ (4-peia = *N*-(2-pyridin-4-ylethyl)isonicotinamide), complementary amide···amide hydrogen bonds effectively connect each square grid. Compared with symmetrical amide- or urea-containing ligands, these types of unsymmetrical amide-containing ligands have not yet been employed widely in a systematic manner.

To establish principles, researchers often exploit a simple system that allows modeling and study of phenomena that are superimposed upon a more complicated, multicomponent system. Thus, one-dimensional (1D) chainlike complexes, being the simplest topological type of coordination array, represent a good starting point to model and investigate infinite, polymeric compounds to develop strategies for engineering supramolecular polymers. In this paper, to explore the contribution of py-CONH-(CH_2)-py-type ligands, crystal structures of coordination networks based on *N*-(4-pyridyl)isonicotinamide (4-pia), *N*-(pyridin-4-ylmethyl)isonicotinamide (4-pmia), *N*-(pyridin-3-ylmethyl)isonicotinamide (3-pmia), and *N*-(pyridin-4-ylmethyl)nicotinamide (4-pmna) are shown. By fixing the metal coordination geometry as linear, we have explored the solid structures resulting from reactions of AgX ($X = PF_6^-$, ClO_4^-, BF_4^-, and NO_3^-) with the above-mentioned ligands.

Results and Discussion

Design strategy: The systems mentioned in this paper operate under conditions in which distinct metal coordination and hydrogen bonds should be involved in independent binding events between unsymmetrical amide-containing ligands and AgX ($X = PF_6^-$, ClO_4^-, BF_4^-, and NO_3^-). Scheme 2 shows our proposed amide-containing py-X-py-type ligands. These ligands consist of three structural parts: 1) pyridyl groups that can coordinate to a metal, 2) an amide group that can form hydrogen-bond interactions with nitrogen and oxygen atoms, and 3) an alkyl moiety that can lengthen the ligands. Due to their unsymmetrical shapes, two kinds of N donors, nitrogen atoms in the carbonyl pyridine (N^C) and those in the amino (or methylene) pyridine (N^N or N^M), are available. Because of π conjugation between the carbonyl pyridine and the amide moiety, nearly zero torsion angles between their planes are expected. This results in the following four ligand shapes in coordination networks: rod, arch, L-shape, and zigzag (Scheme 2), such as 4,4′-bipyridine (4,4′-bpy), 3,4′-bipyridine (3,4′-bpy), and 3,3′-bipyridine (3,3′-bpy).

The coordination sphere of Ag^I can adopt coordination numbers between two and six[11,12] and prefers a linear two-coordinate geometry with N donor ligands to afford 1D chains with bidentate py-X-py-type ligands.[13] Amide moieties in the ligands would guide hydrogen-bonding interactions among 1D chains; it is expected that each chain would be cross-linked by the complementary amide···amide hydrogen bonds, or intermolecular hydrogen bonds by means of anions or solvent molecules.

Crystal structures of $\{[Ag(4\text{-pia})][X]\}_n$ (1⊃X; X = PF_6^-, ClO_4^-, BF_4^-, and NO_3^-): $\{[Ag(4\text{-pia})][PF_6]\}_n$ (1⊃PF_6^-) comprises one Ag^I atom and one 4-pia ligand that are crystallo-

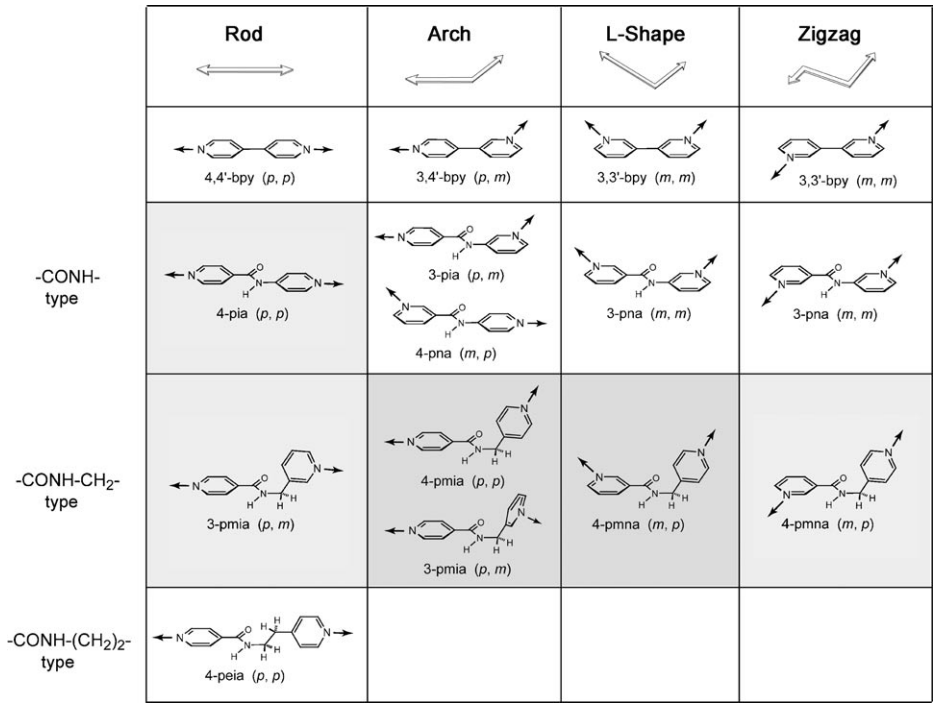

Scheme 2. The amide-containing py-X-py-type ligands used in this study, which result in rod, arch, L, and zigzag ligand shapes in coordination networks. *m* and *p* signify *meta* and *para*, respectively.

graphically independent (Figure 1a). The 4-pia ligands are linked by Ag^I atoms to produce a 1D network. Each Ag^I atom is coordinated by two pyridine nitrogen atoms of 4-pia ligands of the N^C and N^N types, leading to an electronically unsymmetrical Ag^I center. All chains run along the $(a+c)$ direction, with pyridine rings perpendicular to the *ac* plane. Adjacent chains run in opposite directions, as shown in Figure 1b. The 1D chains are not linear but wavy; Ag^I atoms are at the top and bottom of the waves. Between the two parallel chains, the closest approach is Ag^I–Ag^I at 3.622(1) Å, whereas the greatest separation is around PF_6^- anions at about 7.1 Å. The PF_6^- anions are weakly associated with the Ag^I atoms (Ag^I–F = 2.764(7) Å) and are hydrogen bonded to amide moieties (N-(amide)···F = 3.00(1) Å). Despite close amide–amide distances between the chains (N–O = 3.203(8) Å), the hydrogen bonds between PF_6^- and amide moieties obstruct the formation of amide···amide hydrogen bonds.

Although the anions exhibit substantial differences in both shape and size (molecular sizes: PF_6^- = 54 Å^3, ClO_4^- = 47 Å^3, BF_4^- = 38 Å^3, and NO_3^- = 34 Å^3),[14] $\{[Ag(4\text{-pia})][ClO_4]\}_n$ (**1**⊃ClO_4^-), $\{[Ag(4\text{-pia})][BF_4]\}_n$ (**1**⊃BF_4^-), and $\{[Ag(4\text{-pia})][NO_3]\}_n$ (**1**⊃NO_3^-), adopt similar network motifs to **1**⊃PF_6^- (Figure 2). In **1**⊃ClO_4^-, **1**⊃BF_4^-, and **1**⊃NO_3^-, all wavy 1D chains run along the $(a+c)$ direction with adjacent chains running in the opposite direction, as in **1**⊃PF_6^-. Table 1 summarizes selected bond lengths and angles within four compounds of **1**. Coordination distances and angles around Ag^I atoms are similar. As with PF_6^- molecules in **1**⊃PF_6^-, each anion in the network is hydrogen bonded to amide

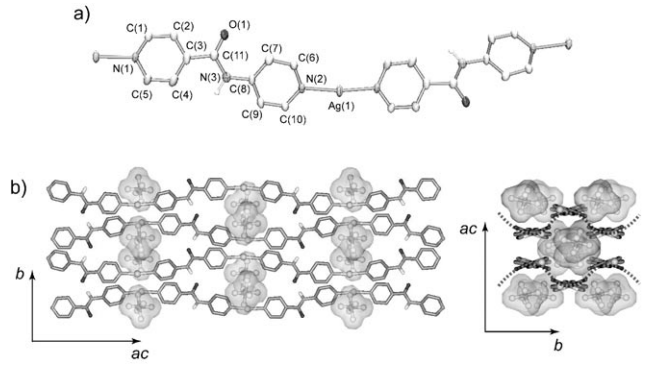

Figure 1. Crystal structures of $\{[Ag(4\text{-pia})][PF_6]\}_n$ (**1**⊃PF_6^-). a) ORTEP drawing of **1**⊃PF_6^- at the 30% probability level. The PF_6^- ion and hydrogen atoms except for those of the amide hydrogen are omitted for clarity. b) Overall structure (left) and cross-sectional view (right) of **1**⊃PF_6^-. 1D chains run in parallel to form a sheet, in which PF_6^- ions are accommodated. Dotted lines (right) correspond to sheets.

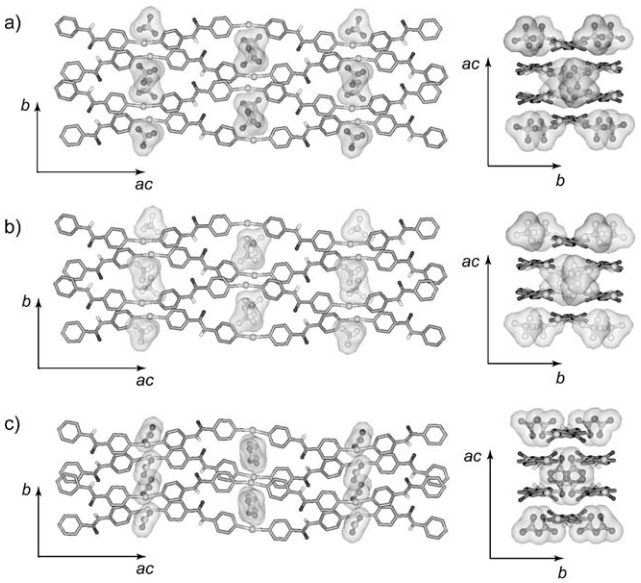

Figure 2. Crystal structures (left) and cross-sectional views (right) of a) $\{[Ag(4\text{-pia})][ClO_4]\}_n$ (**1**⊃ClO_4^-), b) $\{[Ag(4\text{-pia})][BF_4]\}_n$ (**1**⊃BF_4^-), and c) $\{[Ag(4\text{-pia})][NO_3]\}_n$ (**1**⊃NO_3^-). Hydrogen atoms except for those in amide moieties are omitted for clarity. 1D chains run in parallel to form a sheet.

Table 1. Selected bond lengths [Å] and angles [°] in **1**⊃X (X = PF_6^-, ClO_4^-, BF_4^-, and NO_3^-).

	Ag–N^C	Ag–N^N	N^C-Ag-N^N	Ag–Ag	O(amide)–N(amide)
1⊃PF_6^-	2.122(5)	2.110(5)	172.1(2)	3.622(1)	3.203(8)
1⊃ClO_4^-	2.139(8)	2.147(8)	168.1(3)	3.293(2)	3.35(1)
1⊃BF_4^-	2.144(4)	2.140(4)	169.2(2)	3.2692(7)	3.361(7)
1⊃NO_3^-	2.167(3)	2.155(3)	168.4(1)	3.2824(9)	3.135(5)

moieties. Thus, **1**⊃ClO_4^-, **1**⊃BF_4^-, and **1**⊃NO_3^- also do not contain complementary amide···amide hydrogen bonds.

Crystal structures of {[Ag(4-pmia)][X]}$_n$ (2⊃X; X=PF_6^-, ClO_4^-·H_2O, and NO_3^-·H_2O): Figure 3 shows the crystal structure of {[Ag(4-pmia)][PF_6]}$_n$ (**2**⊃PF_6^-). There are two kinds of individual Ag^I, 4-pmia, and PF_6^- molecule in the crystal. Each Ag^I atom is coordinated by two pyridine nitrogen atoms of 4-pmia molecules, N^C and N^M. Although these pyridine donors are nonequivalent because of the unsymmetrical structure of this ligand, the two Ag^I–N bond lengths are similar: Ag^I–N^C = 2.160(5) and 2.152(5) Å, Ag^I–N^M = 2.152(5) and 2.134(6) Å (Table 2). Coordination of the two types of pyridine donor in 4-pmia ligands affords a slightly bent geometry (N^C-Ag^I-N^M = 161.0(2) and 162.0(2)°). Each Ag^I atom is linked by the 4-pmia ligands to provide a 1D chain of {[Ag(4-pmia)][PF_6]}$_n$, which forms a zigzag shape, turning at the methylene moiety (angles (N-(amide)-C(methyl)-C(pyridine)) = 113.6(5) and 114.7(5)°).

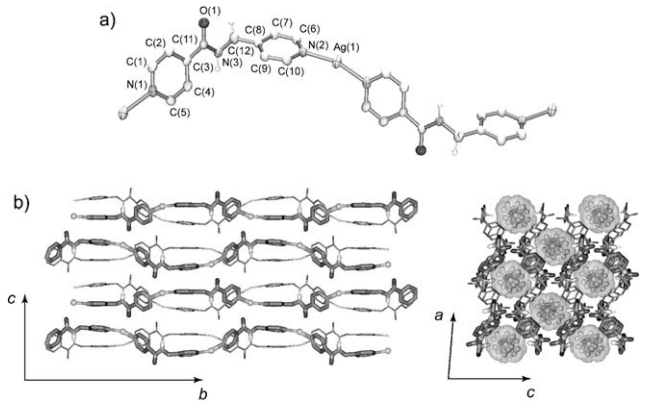

Figure 3. Crystal structures of {[Ag(4-pmia)][PF_6]}$_n$ (**2**⊃PF_6^-). a) ORTEP drawing of **2**⊃PF_6^- at the 30% probability level. The PF_6^- ion and hydrogen atoms of pyridine rings are omitted for clarity. b) Overall structure (left) and cross-sectional view (right) of **2**⊃PF_6^-. 1D chains run in parallel to form a sheet with C=O–Ag^I interactions. Two sheets stack, and the thin and thick lines show the upper and lower sheets, respectively.

Table 2. Selected bond lengths [Å] and angles [°] in **2**⊃X (X = PF_6^-, ClO_4^-·H_2O, and NO_3^-·H_2O).

	Ag–N^C	Ag–N^M	N^C-Ag-N^M
2⊃PF_6^-	2.160(5), 2.152(5)	2.152(5), 2.134(6)	161.0(2), 162.0(2)
2⊃ClO_4^-·H_2O	2.165(5)	2.163(5)	174.6(2)
2⊃NO_3^-·H_2O	2.163(3)	2.159(3)	173.3(1)

The direction of each chain (-[NH-$(CH_2)_n$-py-Ag-py-CO]- or -[CO-py-Ag-py-$(CH_2)_n$-NH]-) is opposite to that of neighboring chains. These chains are aligned along the *c* axis and slide against neighboring chains, where oxygen atoms in amide moieties interact with Ag^I atoms[13c–e] (Ag^I–O(amide) = 2.611(5) and 2.685(5) Å) to form wave sheets (Figure 3b). These sheets are stacked along the *a* axis to afford 1D channels filled with PF_6^- molecules as shown in Figure 3b.

As well as **2**⊃PF_6^-, in {[Ag(4-pmia)][ClO_4]·H_2O}$_n$ (**2**⊃ClO_4^-·H_2O) and {[Ag(4-pmia)][NO_3]·H_2O}$_n$ (**2**⊃NO_3^-·H_2O) each Ag^I atom is coordinated by two pyridine nitrogen atoms of 4-pmia molecules, N^C and N^M, to afford wavy 1D chains. Each chain direction is opposite to that of neighboring chains, as shown in Figure 4. The packing modes of chains found in **2**⊃ClO_4^-·H_2O and **2**⊃NO_3^-·H_2O are different from those in **2**⊃PF_6^-. Oxygen atoms of amide moieties in both **2**⊃ClO_4^-·H_2O and **2**⊃NO_3^-·H_2O project from the chain and hydrogen bond to water molecules. Incorporated water molecules are hydrogen bonded to three surrounding sites, namely oxygen atoms in amide moieties, oxygen atoms in anions, and hydrogen atoms in amide moieties. As shown in Figure 4, ClO_4^- and NO_3^- ions interact with Ag^I atoms and are placed among these zigzag chains.

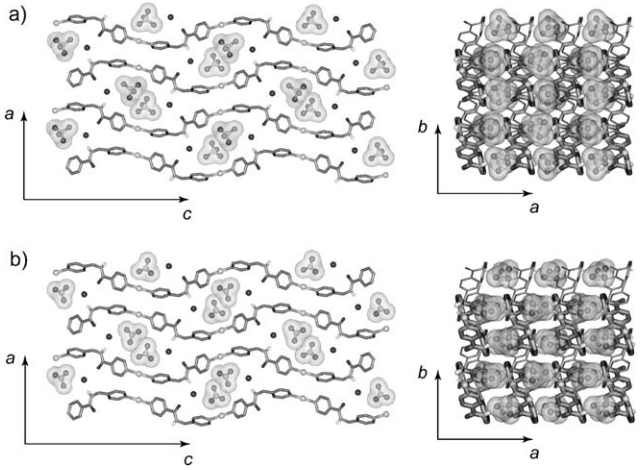

Figure 4. Overall structures (left) and cross-sectional views (right) of 1D chains of a) {[Ag(4-pmia)][ClO_4]·H_2O}$_n$ (**2**⊃ClO_4^-·H_2O) and b) {[Ag(4-pmia)][NO_3]·H_2O}$_n$ (**2**⊃NO_3^-·H_2O). 1D chains run in parallel to form a sheet with O(amide)···O(water)···N(amide) hydrogen bonds.

Crystal structures of {[Ag(3-pmia)][X]}$_n$ (3⊃X; X=PF_6^-, ClO_4^-, BF_4^-, and NO_3^-·H_2O): In {[Ag(3-pmia)][PF_6]}$_n$ (**3**⊃PF_6^-), each Ag^I atom is bridged by a 3-pmia ligand with distorted linear geometry (N^C-Ag^I-N^M = 174.9(1)°, Ag^I–N^C = 2.149(3) Å, and Ag^I–N^M = 2.143(3) Å), as shown in Figure 5a, to afford an infinite zigzag chain as in **1** and **2**. Also

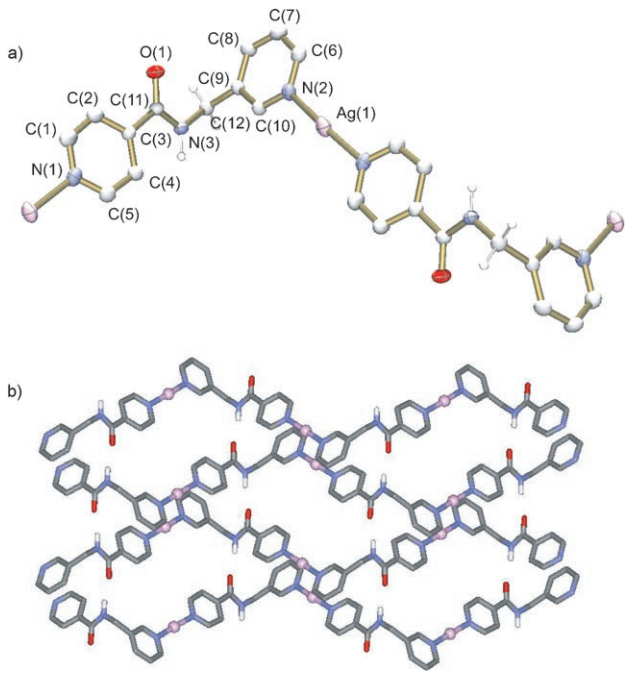

Figure 5. Crystal structures of $\{[Ag(3\text{-pmia})][PF_6]\}_n$ ($\mathbf{3}\supset PF_6^-$). a) ORTEP drawing of $\mathbf{3}\supset PF_6^-$ at the 30% probability level. The PF_6^- anion and hydrogen atoms of pyridine rings are omitted for clarity. b) Overall structure of $\mathbf{3}\supset PF_6^-$. 1D chains run in parallel to form a sheet with O(amide)···HN(amide) hydrogen bonds.

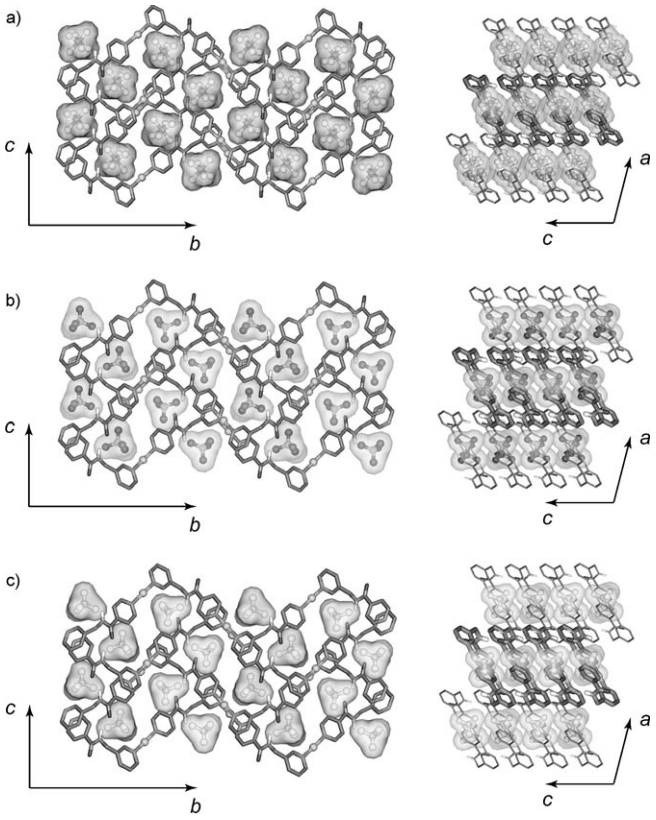

Figure 6. The β-sheet-type structures (left) and their cross-sectional views (right) of a) $\{[Ag(3\text{-pmia})][PF_6]\}_n$ ($\mathbf{3}\supset PF_6^-$), b) $\{[Ag(3\text{-pmia})][ClO_4]\}_n$ ($\mathbf{3}\supset ClO_4^-$), and c) $\{[Ag(3\text{-pmia})][BF_4]\}_n$ ($\mathbf{3}\supset BF_4^-$). Three β sheets are stacked along the *a* axis; thin and thick lines express individual sheets.

in $\mathbf{3}\supset PF_6^-$, each chain direction (-[NH-$(CH_2)_n$-py-Ag-py-CO]- or -[CO-py-Ag-py-$(CH_2)_n$-NH]-) is opposite to that of neighboring chains. It is worth noting that hydrogen bonds of the type NH···O=C (N···O = 2.831(4) Å) existing between the adjacent chains create a complementary amide binding network like a β sheet (Figure 5b). The β sheet of $\mathbf{3}\supset PF_6^-$ is a wavelike sheet with about 10 Å thickness. The closest Ag^I–Ag^I distance between chains is 3.5764(9) Å. These wavelike sheets interdigitate along the *a* axis (Figure 6a), by stacking of methyl pyridine rings with about 4 Å separation. There is no hydrogen bonding between adjacent sheets. Compounds $\{[Ag(3\text{-pmia})][ClO_4]\}_n$ ($\mathbf{3}\supset ClO_4^-$) and $\{[Ag(3\text{-pmia})][BF_4]\}_n$ ($\mathbf{3}\supset BF_4^-$) are isostructural with $\mathbf{3}\supset PF_6^-$, and also form structures like a β sheet, as shown in Figure 6. As Table 3 shows, the amide···amide (N···O) hydrogen-bond lengths between adjacent chains are 2.829(4) and 2.823(4) Å in $\mathbf{3}\supset ClO_4^-$ and $\mathbf{3}\supset BF_4^-$, respectively. Complementary amide···amide hydrogen bonds afford 1D dipole arrays, in which neighboring arrays with opposite directions cancel out. Anion molecules (PF_6^-, ClO_4^-, and BF_4^-) are accommodated within the basins of β sheets.

Table 3. Selected bond lengths [Å] and angles [°] in $\mathbf{3}\supset X$ (X = PF_6^-, ClO_4^-, BF_4^-, and $NO_3^-\cdot H_2O$).

	Ag–N^C	Ag–N^N	N^C-Ag-N^N	Ag–Ag	O(amide)···N(amide)
$\mathbf{3}\supset PF_6^-$	2.149(3)	2.143(3)	174.9(1)	3.5764(9)	2.831(4)
$\mathbf{3}\supset ClO_4^-$	2.162(3)	2.156(3)	172.9(1)	3.3214(7)	2.829(4)
$\mathbf{3}\supset BF_4^-$	2.136(3)	2.144(3)	173.5(1)	3.342(1)	2.823(4)
$\mathbf{3}\supset NO_3^-\cdot H_2O$	2.161(2)	2.159(2)	172.25(8)	–	–

In the case of $\{[Ag(3\text{-pmia})][NO_3]\cdot H_2O\}_n$ ($\mathbf{3}\supset NO_3^-\cdot H_2O$), water molecules are included in the network, since the NO_3^- anion is smaller than other anions.[14] The water molecules are hydrogen bonded to oxygen atoms of amide moieties, oxygen atoms of nitrate anions, and nitrogen atoms in amide moieties (Figure 7), thus affording sheets with intermolecular hydrogen bonds like $\mathbf{2}\supset ClO_4^-\cdot H_2O$ and $\mathbf{2}\supset NO_3^-\cdot H_2O$.

Crystal structures of $\{[Ag(4\text{-pmna})][PF_6]\cdot MeOH\}_n$ ($\mathbf{4a}\supset PF_6^-\cdot MeOH$ and $\mathbf{4b}\supset PF_6^-\cdot MeOH$): In $\{[Ag(4\text{-pmna})](PF_6)\cdot MeOH\}_n$ ($\mathbf{4a}\supset PF_6^-\cdot MeOH$), each Ag^I atom is linearly coordinated to 4-pmna ligands (N^C-Ag^I-N^M = 178.1(1)°, Table 4) to provide a 1D chain. In spite of the nonequivalent pyridine donors, no significant difference was observed for the two Ag^I–N bond lengths: Ag^I–N^C = 2.16(2) and Ag^I–N^M = 2.14(1) Å. The interesting feature of this chain is a helical framework with a 28 Å unit repeated along the *c* axis (Figure 8). Compound $\mathbf{4a}\supset PF_6^-\cdot MeOH$ crystallizes in space group $P4_3$, resulting in a unique single left-handed helical structure. Compound $\mathbf{4a}\supset PF_6^-\cdot MeOH$ has a 4_3 axis

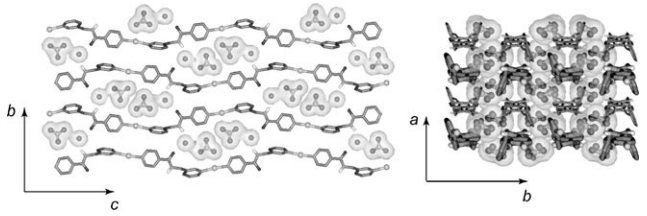

Figure 7. Crystal structures of $\{[Ag(3\text{-pmia})][NO_3]\cdot H_2O\}_n$ ($\mathbf{3}\supset NO_3^-\cdot H_2O$). Overall structure (left) and cross-sectional view (right) of $\mathbf{3}\supset NO_3^-\cdot H_2O$. 1D chains run in parallel to form a sheet with O(amide)···O(water)···N(amide) hydrogen bonds.

Table 4. Selected bond lengths [Å] and angles [°] in $\mathbf{4a}\supset PF_6^-\cdot$MeOH and $\mathbf{4b}\supset PF_6^-\cdot$MeOH.

	$Ag-N^C$	$Ag-N^M$	N^C-Ag-N^M
$\mathbf{4a}\supset PF_6^-\cdot$MeOH	2.16(2)	2.14(1)	178.1(1)
$\mathbf{4b}\supset PF_6^-\cdot$MeOH	2.17(1)	2.13(1)	178.5(5)

along the *c* axis. The PF_6^- ions and methanol molecules are located within the helical columns with close contact distances: Ag^I–O(MeOH) = 2.76(2) and Ag^I–F(PF_6^-) = 3.11(4) Å. One helical column is interdigitated with adjacent columns by weak association between the oxygen atom of the amide moiety and the Ag^I atom in the adjacent chain (Ag^I–O(amide) = 2.78(5) Å).[13c–e] It is well known that the helical structure of proteins is mainly driven and stabilized by intramolecular hydrogen-bonding interactions between amide groups within the flexible polypeptide backbone.[10] However, in $\mathbf{4a}\supset PF_6^-\cdot$MeOH, carbonyl oxygen atoms do not hydrogen bond to N–H, but interact weakly with Ag^I atoms in neighboring chains, unlike the α-helix form in proteins. However, in the case of $\mathbf{4b}\supset PF_6^-\cdot$MeOH, the compound crystallizes in space group $P4_1$, resulting in single right-handed helicity (Figure 8b). Thus, compound **4** crystallizes as cocrystals of $\mathbf{4a}\supset PF_6^-\cdot$MeOH and $\mathbf{4b}\supset PF_6^-\cdot$MeOH.

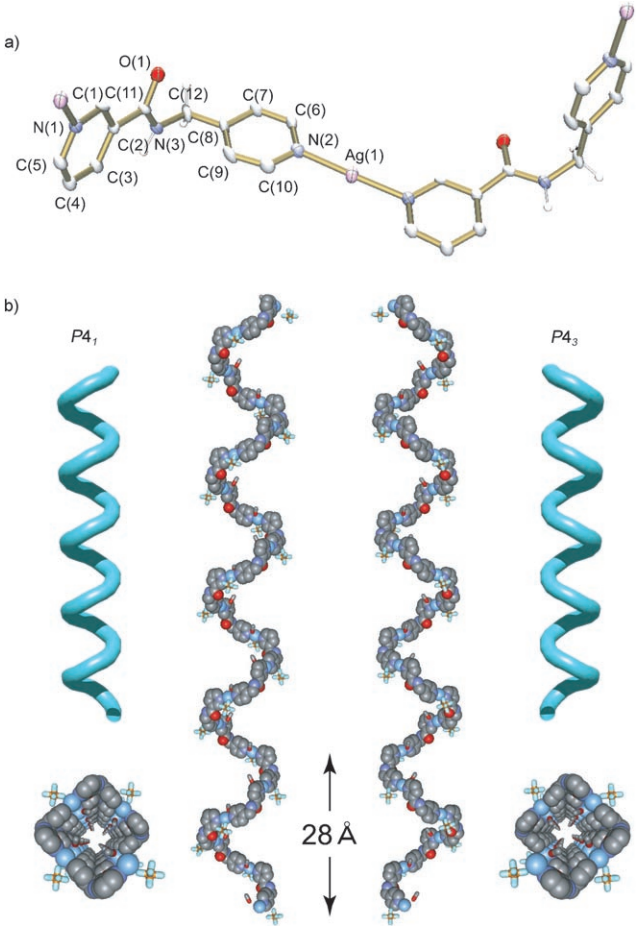

Figure 8. Crystal structures of $\{[Ag(4\text{-pmna})][PF_6]\cdot$MeOH$\}_n$ ($\mathbf{4a}\supset PF_6^-\cdot$MeOH and $\mathbf{4b}\supset PF_6^-\cdot$MeOH). a) ORTEP drawing of $\mathbf{4a}\supset PF_6^-\cdot$MeOH at the 30% probability level. The PF_6^- anion and hydrogen atoms of pyridine rings are omitted for clarity. b) Overall structure of $\mathbf{4a}\supset PF_6^-\cdot$MeOH (right) and $\mathbf{4b}\supset PF_6^-\cdot$MeOH (left). Both compounds form helical structures ($\mathbf{4a}\supset PF_6^-\cdot$MeOH: left-handed; $\mathbf{4b}\supset PF_6^-\cdot$MeOH: right-handed) with the helical pitch of 28 Å.

Comparison of relationship between chains in compounds 1–4: All compounds **1**–**4** form 1D chains, which are attributed to the bridging of Ag^I atoms with linear coordination environments. The most significant feature is that Ag^I atoms are unsymmetrically coordinated in all compounds; that is, N^C-Ag-$N^{N(M)}$, rather than N^C-Ag-N^C and N^N-Ag-N^N (or N^M-Ag-N^M). This coordination mode induces chain direction within -[NH-$(CH_2)_n$-py-Ag-py-CO]- (n = 0 (**1**) or 1 (**2**–**4**)) as seen in amino acid sequences in proteins.[10]

Scheme 3 summarizes the relationships between chains in compounds **1**–**4**. Each chain in compounds **1**–**3** runs parallel, with neighboring chains running in opposite directions. As mentioned previously, amide moieties in **1** form hydrogen bonds with incorporated anion molecules, resulting in no significant interaction between chains. On the other hand, chains are cross-linked with neighboring chains by intermolecular (H_2O) hydrogen bonds in $\mathbf{2}\supset ClO_4^-\cdot H_2O$, $\mathbf{2}\supset NO_3^-\cdot H_2O$, and $\mathbf{3}\supset NO_3^-\cdot H_2O$, and with β-sheet motifs occurring in $\mathbf{3}\supset PF_6^-$, $\mathbf{3}\supset ClO_4^-$, and $\mathbf{3}\supset BF_4^-$.

In proteins, the chain of amino acids produces secondary structures, namely α-helix and β-sheet motifs.[10] The β-sheet structure is classified into two types: parallel and antiparallel.[10] In the former, all chains are oriented in the same direction. In the latter, adjacent chains are oriented in the opposite direction, and folding of a single chain is often observed. The arrangements of hydrogen-bonding linkage in $\mathbf{3}\supset PF_6^-$, $\mathbf{3}\supset ClO_4^-$, and $\mathbf{3}\supset BF_4^-$ is of the latter, antiparallel type.

To date, helical structures based on coordination compounds designed by selecting suitable metals and oligopyridines have been reported,[15] and control of their length and single-, double-, or triple-stranded nature has been achieved.[16] Moreover, β-sheet structures have been obtained by cross-linking 1D coordination polymers.[6a,9f,g,i] Interestingly, in our case, helical and β-sheet structures similar to the self-assembled structures of folded proteins have been obtained from two isomeric py-CONH-(CH_2)-py-type ligands.

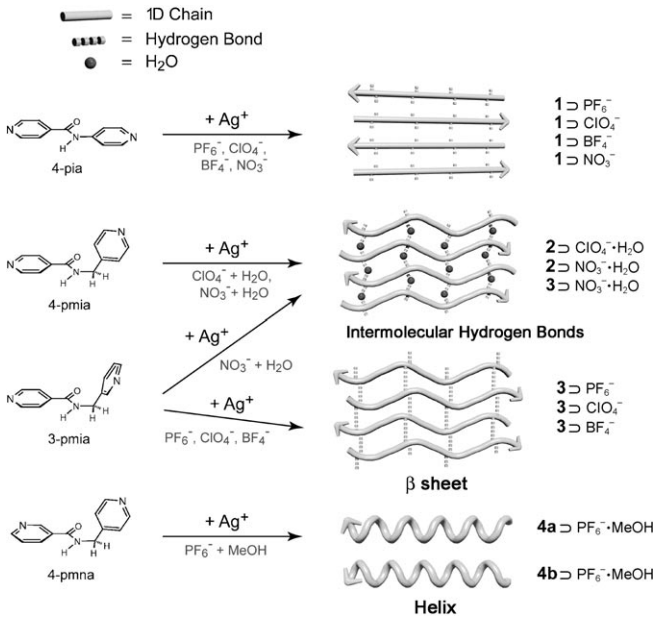

Scheme 3. Summary of the relationships between chains in compounds **1**–**4**.

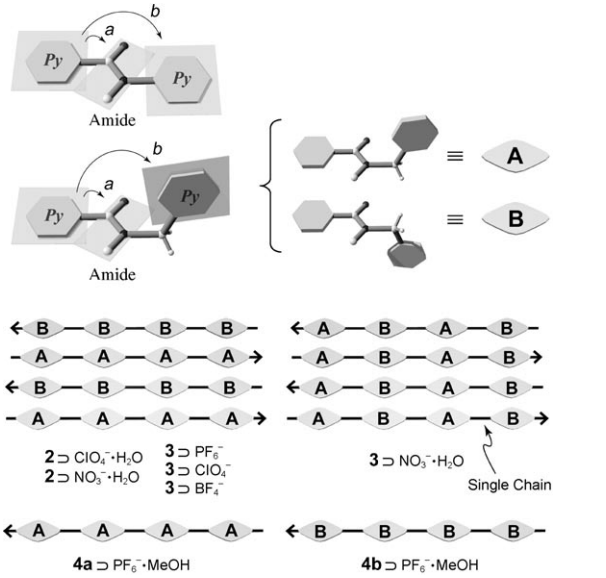

Scheme 4. Scheme showing the three flat planes of the amide-containing ligands, the torsion angles, *a* and *b*, and the two types of confomation, A and B, of the py-CONH-(CH_2)-py-type ligands in compounds **1**–**4**.

Comparison of ligand conformations in compounds 1–4: Amide-containing ligands have three flat planes, the carbonyl pyridine, amino (methylene) pyridine, and amide planes, with each plane connected through single bonds. As shown in Scheme 4, two torsion angles, *a* and *b*, are defined: angle *a* between the carbonyl pyridine and amide plane and angle *b* between the carbonyl pyridine and amino (methylene) pyridine. Table 5 summarizes angles *a* and *b* found in **1**–**4**. A tendency for a large value of *a* to be accompanied by a small value of *b* can be observed.[17] As shown in previous reports,[9i,18] amide···amide hydrogen bonding occurs only when the angle between carbonyl pyridine and the amide plane is greater than 20°. In our case, the *a* angles in **3**⊃PF_6^-, **3**⊃ClO_4^-, and **3**⊃BF_4^- are greater than 20°.

The significant difference among compounds **2**–**4** is the conformation of py-CONH-(CH_2)-py-type ligands, in which two types, A and B, are present. Types A and B imply that the methylene pyridine is on either the upper or lower side relative to the plane of carbonyl pyridine and amide moiety, respectively (Scheme 4). As shown in Scheme 4, in compounds **2** and **3** (except for **2**⊃PF_6^- and **3**⊃NO_3^-·H_2O), all ligand conformations in a single chain are the same, and the two kinds of chain are alternately aligned. Also, in **4a**⊃PF_6^-·MeOH and **4b**⊃PF_6^-·MeOH, only type A or B is crystallized, which induces helical structures. On the other hand, in a single chain of **3**⊃NO_3^-·H_2O, types A and B are alternately connected in the form -A-B-A-B-.[19] Figure 9 shows three kinds of single chain in **2**⊃ClO_4^-·H_2O, **3**⊃ClO_4^-, and **3**⊃NO_3^-·H_2O. Each chain forms a zigzag with pitches of 25.1, 18.9, and 26.6 Å, respectively. It is worth noting that the chain pitch is rationally regulated by the change from *para*- to *meta*-methylene pyridine between **2**⊃ClO_4^-·H_2O and **3**⊃ClO_4^-. Compared with **2**⊃ClO_4^-·H_2O and **3**⊃ClO_4^-, the chain of **3**⊃NO_3^-·H_2O is close to a straight line, which is attributed to the alternating alignment of ligand conformations (-A-B-A-B-).

Table 5. The angles [°] of *a* and *b*, and symbols found in **1**⊃X (X = PF_6^-, ClO_4^-, BF_4^-, and NO_3^-), **2**⊃X (X = PF_6^-, ClO_4^-·H_2O, and NO_3^-·H_2O), **3**⊃**X** (X = PF_6^-, ClO_4^-, BF_4^-, and NO_3^-·H_2O), **4a**⊃PF_6^-·MeOH, and **4b**⊃PF_6^-·MeOH.

	(a,b)[a,b]	Symbol[c]
1⊃PF_6^-	(+27.6, +31.5), (−27.6, −31.5)	C[$Ag^1(p^0, p^0)$]
1⊃ClO_4^-	(+27.0, +29.7), (−27.0, −29.7)	C[$Ag^1(p^0, p^0)$]
1⊃BF_4^-	(+25.8, +26.7), (−25.8, −26.7)	C[$Ag^1(p^0, p^0)$]
1⊃NO_3^-	(+36.2, +18.8), (−36.2, −18.8)	C[$Ag^1(p^0, p^0)$]
2⊃PF_6^-	(+11.7, +66.2), (−11.7, −66.2), (−32.4, +64.5), (+32.4, −64.5)	C[$Ag^1(p^1, p^0)$]
2⊃ClO_4^-·H_2O	(+2.1, +82.5), (−2.1, −82.5)	C[$Ag^1(p^1, p^0)$]
2⊃NO_3^-·H_2O	(+3.2, +76.7), (−3.2, −76.7)	C[$Ag^1(p^1, p^0)$]
3⊃PF_6^-	(+22.0, +64.8), (−22.0, −64.8)	C[$Ag^1(m^1, p^0)$]
3⊃ClO_4^-	(+20.9, +65.3), (−20.9, −65.3)	C[$Ag^1(m^1, p^0)$]
3⊃BF_4^-	(+21.0, +62.7), (−21.0, −62.7)	C[$Ag^1(m^1, p^0)$]
3⊃NO_3^-·H_2O	(+7.3, +73.6), (−7.3, −73.6)	C[$Ag^1(m^1, p^0)$]
4a⊃PF_6^-·MeOH	(−5.0, +90.0)	C[$Ag^1(p^1, m^0)$]
4b⊃PF_6^-·MeOH	(+5.6, −89.6)	C[$Ag^1(p^1, m^0)$]

[a] *a* = angle (Py(carbonyl)–amide plane). [b] *b* = angle (Py(carbonyl)–Py(amino or methylene)). [c] Symbols are assigned according to our previously reported category in which the NH-py-M-py-CO unit in a "metallo-amino acid" was regarded as an "amino acid fragment". See ref. [4]. C: chain (designator of patterns); *m* and *p*: *meta* and *para* (substituted position of NH- or CO-containing group); 0 and 1: number of atoms in between NH- (or CO-) and py group.

The most interesting feature in our system is that two kinds of biomimetic structure, the β sheet and the helix, have been constructed by combining py-CONH-CH_2-py-type ligands with $AgPF_6$. A slight change of ligand orientation, (*para*-N^C, *meta*-N^M) and (*meta*-N^C, *para*-N^M), induces drastic structural difference, namely β sheet (**3**⊃PF_6^-,

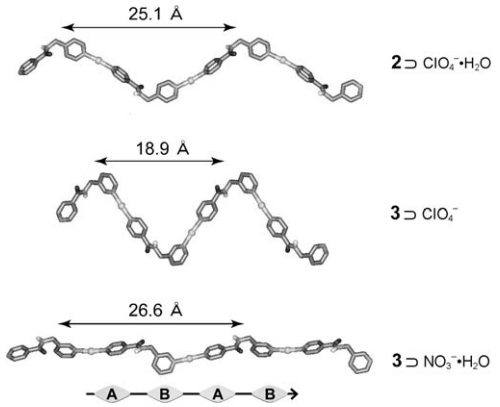

Figure 9. Single chains of $\{[Ag(4\text{-pmia})][ClO_4]\cdot H_2O\}_n$ ($\mathbf{2}\supset ClO_4^-\cdot H_2O$), $\{[Ag(3\text{-pmia})][ClO_4]\}_n$ ($\mathbf{3}\supset ClO_4^-$), and $\{[Ag(3\text{-pmia})][NO_3]\cdot H_2O\}_n$ ($\mathbf{3}\supset NO_3^-\cdot H_2O$) with schematic views.

$\mathbf{3}\supset ClO_4^-$, and $\mathbf{3}\supset BF_4^-$) and helix ($\mathbf{4a}\supset PF_6^-\cdot$MeOH and $\mathbf{4b}\supset PF_6^-\cdot$MeOH). Scheme 5 shows single chains of $\mathbf{3}\supset PF_6^-$ and $\mathbf{4a}\supset PF_6^-\cdot$MeOH, in which both have -A-A-A-A- ligand alignments with arch- and L-shaped networks, respectively. The drastic difference is attributed to the torsion angles between two ligands through the Ag^I atoms. In $\mathbf{3}\supset PF_6^-$, the torsion angles are about 180°, with amide moieties directly opposed. On the other hand, in $\mathbf{4a}\supset PF_6^-\cdot$MeOH, the torsion angles are about 0°, which produces a 4_3 helical structure. As shown in Scheme 5, the schematic drawing of $\mathbf{3}\supset PF_6^-$ with torsion angles of 0° exhibits the helical form, thus compound **3** also potentially has the possibility of helical crystal structures with additional molecules such as MeOH in $\mathbf{4a}\supset PF_6^-\cdot$MeOH.

Anion binding and irreversible anion exchange with structural transformation: Recent investigations of anion recognition[20] have revealed that urea moieties in molecules are good candidates for anion binding and focused also on amide moieties.[20e] In all compounds **1**–**3**, each anion is surrounded by and packed between 1D chains, within which

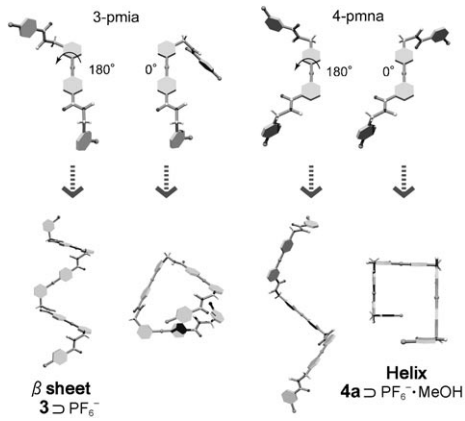

Scheme 5. The single chains of $\mathbf{3}\supset PF_6^-$ and $\mathbf{4a}\supset PF_6^-\cdot$MeOH, in which both have -A-A-A-A- ligand alignments with arch- and L-shaped networks, respectively.

Ag^I atoms and amide moities interact at close proximity. To compare experimentally the thermodynamic stabilities for crystal-packing forces, heterogeneous anion exchanges[9c,h,13c,d,21] were carried out. The experiments were performed as follows: freshly bulk-synthesized powder samples (0.50 mmol) were immersed in aqueous solutions (5 mL) containing excess NaX ($X = PF_6^-$, ClO_4^-, BF_4^-, or NO_3^-; 25 mmol) for three days. The resulting powder samples were filtered, washed with water, and dried in air, followed by measurement of IR spectra and X-ray powder diffraction (XRPD).[22] Although anion exchanges may proceed by means of dissolution,[21i] it is possible to compare the stabilities.

In the case of $\mathbf{1}\supset X$ ($X = PF_6^-$, ClO_4^-, BF_4^-, and NO_3^-), anion exchange did not proceed, which indicated that anions in the crystal are closely packed.[23] On the other hand, in $\mathbf{2}\supset X$ ($X = PF_6^-$, $ClO_4^-\cdot H_2O$, or $NO_3^-\cdot H_2O$), the exchanges occurred smoothly by means of crystal-to-crystal transformations and reverse exchange was also observed. Figure 10 shows the anion environments in compounds $\mathbf{2}\supset X$. Anions are in close contact with several Ag^I atoms, and hydrogen bonded to the amide moiety in $\mathbf{2}\supset PF_6^-$, but to water molecules in both $\mathbf{2}\supset ClO_4^-\cdot H_2O$ and $\mathbf{2}\supset NO_3^-\cdot H_2O$. Taking these results into account, paired incorporation (anion and water molecules) affords nonrigid hydrogen-bonded networks in this system. This conclusion is also supported by the results in $\mathbf{3}\supset X$ ($X = PF_6^-$, ClO_4^-, BF_4^-, and $NO_3^-\cdot H_2O$). Compound $\mathbf{3}\supset NO_3^-\cdot H_2O$ was smoothly exchanged to become $\mathbf{3}\supset PF_6^-$, $\mathbf{3}\supset ClO_4^-$, or $\mathbf{3}\supset BF_4^-$ by means of crystal-to-crystal transformations. On the other hand, compounds $\mathbf{3}\supset PF_6^-$ and $\mathbf{3}\supset ClO_4^-$ did not release their incorporated anions from their structures, even when the crystals were immersed in aqueous solutions including excess quantities of other anion-

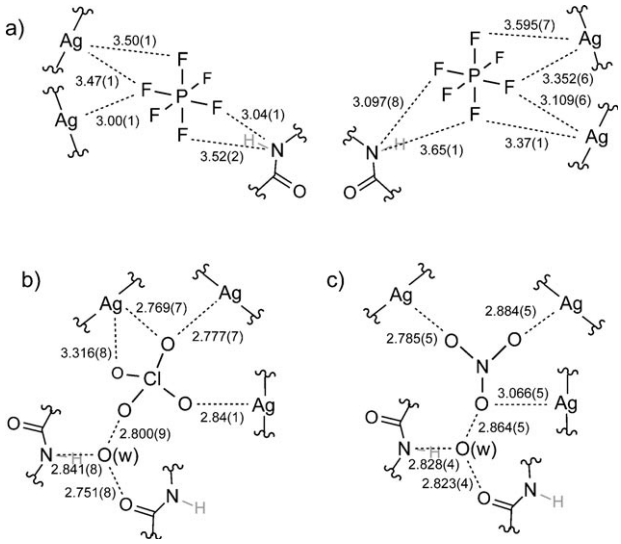

Figure 10. Schematic views of the anion environments in a) $\{[Ag(4\text{-pmia})][PF_6]\}_n$ ($\mathbf{2}\supset PF_6^-$), b) $\{[Ag(4\text{-pmia})][ClO_4]\cdot H_2O\}_n$ ($\mathbf{2}\supset ClO_4^-\cdot H_2O$), and c) $\{[Ag(4\text{-pmia})][NO_3]\cdot H_2O\}_n$ ($\mathbf{2}\supset NO_3^-\cdot H_2O$). Values represent the distances [Å] between atoms. Expressions for double bonds in ClO_4^- and NO_3^- anions are omitted.

ic species.[24] Such irreversible anion exchange indicates that the hydrogen-bonded structure of compounds **3**⊃PF_6^- and **3**⊃ClO_4^- are relatively rigid (Figures 6 and 11), thus indicating that the β-sheet type of structure is rather more stable thermodynamically than the networks of intermolecular hydrogen bonds.

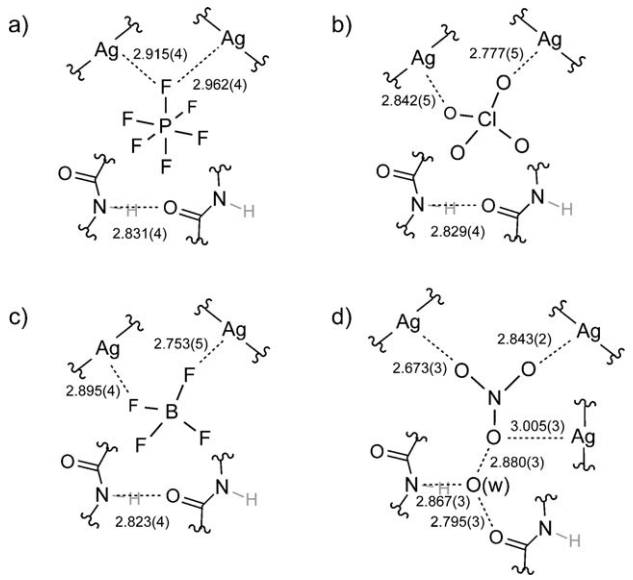

Figure 11. Schematic views of the anion environments in a) {[Ag(3-pmia)][PF_6]}$_n$ (**3**⊃PF_6^-), b) {[Ag(3-pmia)][ClO_4]}$_n$ (**3**⊃ClO_4^-), c) {[Ag(3-pmia)][BF_4]}$_n$ (**3**⊃BF_4^-), and d) {[Ag(3-pmia)][NO_3]·H_2O}$_n$ (**3**⊃NO_3^-·H_2O). Values represent the distances [Å] between atoms. Expressions for double bonds in ClO_4^- and NO_3^- anions are omitted.

Conclusion

In this paper, we have demonstrated that the amide-containing ligands 4-pia, 4-pmia, 3-pmia, and 4-pmna afford 1D chains in combination with Ag^I atoms. Although structural controls in this new topological system of py-CO-NH-CH_2-py are rather difficult because of the free rotation of the methylene moieties, all compounds form chains with unsymmetrical Ag^I coordination environments. Crystal structures show that the amide moieties in the ligands, especially in 3-pmia, project from parallel-aligned chains and participate in cross-linking of chains in the crystals. We have, therefore, developed a series of amide-containing coordination networks that open the way to new possibilities in metal–ligand architectures useful for the construction of linkage networks using complementary amide bindings. This principle of crystal engineering and supramolecular synthesis could be used to design, isolate, and characterize a number of novel network structures that are prototypal.

Experimental Section

Materials: Isonicotinoyl chloride hydrochloride, nicotinoyl chloride hydrochloride, 4-aminopyridine, 3-aminopyridine, 4-(aminomethyl)pyridine, 3-(aminomethyl)pyridine, and $NaPF_6$ were obtained from Tokyo Kasei Industrial Co. $AgNO_3$, $NaNO_3$, and $NaBF_4$ were obtained from Wako Co. $AgPF_6$ was obtained from Aldrich Chemical Co. $AgBF_4$ and $AgClO_4$·$n H_2O$ were obtained from Nacalai Tesque Co. $NaClO_4$ was obtained from Kishida Chemical Co. The 4-pmna was synthesized according to a reported procedure.[8c]

Synthesis of *N*-(pyridin-4-ylmethyl)isonicotinamide (4-pmia): The ligand was prepared by the reaction of isonicotinoyl chloride hydrochloride (13.0 g, 73.0 mmol) with 4-pycolylamine (7.4 mL, 73.0 mmol) in dry tetrahydrofuran (250 mL) in the presence of triethylamine (21 mL, 150 mmol) under N_2. The product was recrystallized from acetone/hexane in 36% yield (5.7 g). ^{1}H NMR (DMSO): $\delta = 4.51$ (d, $J = 6.0$ Hz, 2H), 7.31 (d, $J = 5.5$ Hz, 2H), 7.80 (d, $J = 6.0$ Hz, 2H), 8.50 (d, $J = 5.5$ Hz, 2H), 8.74 (d, $J = 6.0$ Hz, 2H), 9.41 ppm (t, $J = 6.0$ Hz, 1H); elemental analysis calcd (%) for $C_{12}H_{11}N_3O$: C 67.59, H 5.20, N 19.71; found: C 67.39, H 5.25, N 19.58.

Synthesis of *N*-(pyridin-3-ylmethyl)isonicotinamide (3-pmia): The ligand was prepared by the reaction of isonicotinoyl chloride hydrochloride (6.5 g, 36.5 mmol) with 3-pycolylamine (3.7 mL, 36.5 mmol) in dry tetrahydrofuran (125 mL) in the presence of triethylamine (10.5 mL, 75 mmol) under N_2. The product was recrystallized from acetone/hexane in 45% yield (3.5 g). ^{1}H NMR (DMSO): $\delta = 4.51$ (d, $J = 6.0$ Hz, 2H), 7.36 (dd, $J = 8.0$, 5.0 Hz, 1H), 7.73 (d, $J = 8.0$ Hz, 1H), 7.78 (d, $J = 6.0$ Hz, 2H), 8.46 (d, $J = 5.0$ Hz, 1H), 8.56 (s, 1H), 8.73 (d, $J = 6.0$ Hz, 2H), 9.37 ppm (t, $J = 6.0$ Hz, 1H); elemental analysis calcd (%) for $C_{12}H_{11}N_3O$: C 67.59, H 5.20, N 19.71; found: C 67.02, H 5.04, N 19.62.

Synthesis of {[Ag(4-pia)][PF_6]}$_n$ (1⊃PF_6^-): A solution of 4-pia (2.99 mg, 0.015 mmol) in ethanol (1.5 mL) was carefully layered on a solution of $AgPF_6$ (1.90 mg, 0.008 mmol) in water (1.5 mL), with a mixed solvent of ethanol/water (v/v 1:1, 1.5 mL) placed between the two layers (yield: 99%). FTIR: $\tilde{\nu} = 3393$ (m; ν, N–H stretching band), 1694 (s; ν, amide-I), 1518 (s; δ, amide-II), 842 cm^{-1} (s, br; ν, PF_6^-); elemental analysis calcd (%) for $C_{11}H_9AgF_6N_3OP$: C 29.23, H 2.01, N 9.30; found: C 29.37, H 2.16, N 9.31.

Synthesis of {[Ag(4-pia)][ClO_4]}$_n$ (1⊃ClO_4^-): A solution of 4-pia (14.9 mg, 0.075 mmol) in ethanol (1.5 mL) was carefully layered on a solution of $AgClO_4$·$n H_2O$ (7.77 mg, 0.038 mmol) in water (1.5 mL), with a mixed solvent of ethanol/water (v/v 1:1, 1.5 mL) placed between the two layers (yield: 19%). FTIR: $\tilde{\nu} = 3328$ (m; ν, N–H stretching band), 1689 (s; ν, amide-I), 1515 (s; δ, amide-II), 1089 cm^{-1} (s, multibands; ν, ClO_4^-); elemental analysis calcd (%) for $C_{11}H_9AgClN_3O_5$: C 32.50, H 2.23, N 10.34; found: C 32.30, H 2.30, N 10.33.

Synthesis of {[Ag(4-pia)][BF_4]}$_n$ (1⊃BF_4^-): A solution of 4-pia (14.9 mg, 0.075 mmol) in ethanol (1.5 mL) was carefully layered on a solution of $AgBF_4$ (7.30 mg, 0.038 mmol) in water (1.5 mL), with a mixed solvent of ethanol/water (v/v 1:1, 1.5 mL) placed between the two layers (yield: 5.5%). FTIR: $\tilde{\nu} = 3350$ (m; ν, N–H stretching band), 1690 (s; ν, amide-I), 1516 (s; δ, amide-II), 1075 cm^{-1} (s, multibands; ν, BF_4^-); elemental analysis calcd (%) for $C_{11}H_9AgBF_4N_3O$: C 33.54, H 2.30, N 10.67; found: C 33.71, H 2.41, N 10.79.

Synthesis of {[Ag(4-pia)][NO_3]}$_n$ (1⊃NO_3^-): A solution of 4-pia (14.9 mg, 0.075 mmol) in ethanol (1.5 mL) was carefully layered on a solution of $AgNO_3$ (6.37 mg, 0.038 mmol) in water (1.5 mL), with a mixed solvent of ethanol/water (v/v 1:1, 1.5 mL) placed between the two layers (yield: 42%). FTIR: $\tilde{\nu} = 3273$ (m, br; ν, N–H stretching band), 1695 (s; ν, amide-I), 1524 (s; δ, amide-II), 1385 cm^{-1} (s; ν, NO_3^-); elemental analysis calcd (%) for $C_{11}H_9AgN_4O_4$: C 35.80, H 2.46, N 15.18; found: C 35.91, H 2.60, N 15.33.

Synthesis of {[Ag(4-pmia)][PF_6]}$_n$ (2⊃PF_6^-): A solution of 4-pmia (32 mg, 0.15 mmol) in ethanol (1.5 mL) was carefully layered on a solution of $AgPF_6$ (19 mg, 0.075 mmol) in water (1.5 mL), with a mixed solvent of ethanol/water (v/v 1:1) placed between the two layers (yield: 74%). FTIR: $\tilde{\nu} = 3431$ and 3413 (m; ν, N–H stretching band), 1661 (s; ν, amide-I), 1543 (s; δ, amide-II), 842 cm^{-1} (s, br; ν, PF_6^-); elemental analysis calcd (%) for $C_{12}H_{11}AgF_6N_3OP$: C 30.92, H 2.38, N 9.02; found: C 31.62, H 2.44, N 9.53.

Synthesis of {[Ag(4-pmia)][ClO_4]·H_2O}$_n$ (2⊃ClO_4^-·H_2O): A solution of 4-pmia (16 mg, 0.075 mmol) in ethanol (1.5 mL) was gently layered on a

Table 6. Crystal data and structure refinements of **1**⊃PF_6^- **1**⊃ClO_4^-, **1**⊃BF_4^-, **1**⊃NO_3^-, **2**⊃PF_6^-, **2**⊃ClO_4^-·H_2O, **2**⊃NO_3^-·H_2O, **3**⊃PF_6^-, **3**⊃ClO_4^-, **3**⊃BF_4^-, **3**⊃NO_3^-·H_2O, **4a**⊃PF_6^-·MeOH, and **4b**⊃PF_6^-·MeOH.

Compound	**1**⊃PF_6^-	**1**⊃ClO_4^-	**1**⊃BF_4^-	**1**⊃NO_3^-	**2**⊃PF_6^-	**2**⊃ClO_4^-·H_2O	**2**⊃NO_3^-·H_2O
formula	$C_{11}H_9AgF_6N_3OP$	$C_{11}H_9AgClN_3O_5$	$C_{11}H_9BAgF_4N_3O$	$C_{11}H_9AgN_4O_4$	$C_{24}H_{22}Ag_2F_{12}N_6O_2P_2$	$C_{12}H_{11}AgClN_3O_6$	$C_{12}H_{11}AgN_4O_5$
M_r	452.04	406.53	393.88	369.08	932.14	436.56	399.11
crystal system	monoclinic	monoclinic	monoclinic	monoclinic	monoclinic	orthorhombic	orthorhombic
space group	*C*2/*c*	*C*2/*c*	*C*2/*c*	*C*2/*c*	$P2_1/n$	*Pbca*	*Pbca*
T [K]	293	293	293	293	293	293	293
a [Å]	20.222(8)	19.760(10)	19.670(8)	19.67(1)	9.704(4)	13.4092(9)	12.903(5)
b [Å]	8.652(3)	8.112(3)	7.908(3)	6.728(4)	25.40(1)	9.3825(7)	9.022(4)
c [Å]	16.482(6)	16.797(8)	16.980(7)	18.67(1)	12.458(5)	25.048(1)	24.54(1)
α [°]	90	90	90	90	90	90	90
β [°]	92.282(6)	93.519(7)	92.943(6)	91.663(9)	94.893(6)	90	90
γ [°]	90	90	90	90	90	90	90
V [Å^3]	2881(1)	2687(2)	2637(1)	2470(2)	3058(2)	3151.3(3)	2856(2)
Z	8	8	8	8	4	8	8
ρ_{calcd} [g cm^{-1}]	2.084	2.009	1.984	1.985	2.024	1.840	1.856
μ ($Mo_{K\alpha}$) [mm^{-1}]	1.579	1.719	1.572	1.647	1.491	1.478	1.437
2θ range [°]	5.5–55.0	5.5–54.9	5.5–54.9	5.5–55.0	5.5–55.0	5.5–53.4	5.5–54.9
GOF on F^2	1.787	2.896	1.658	1.524	1.734	0.932	1.255
R_1[a] [$I>2\sigma(I)$]	0.070	0.104	0.050	0.044	0.071	0.069	0.048
wR_2[b] (all data)	0.209	0.336	0.140	0.124	0.188	0.240	0.129

Compound	**3**⊃PF_6^-	**3**⊃ClO_4^-	**3**⊃BF_4^-	**3**⊃NO_3^-·H_2O	**4a**⊃PF_6^-·MeOH	**4b**⊃PF_6^-·MeOH
formula	$C_{12}H_{11}AgF_6N_3OP$	$C_{12}H_{11}AgClN_3O_5$	$C_{12}H_{11}BAgF_4N_3O$	$C_{12}H_{11}AgN_4O_5$	$C_{13}H_{11}AgF_6N_3O_2P$	$C_{13}H_{11}AgF_6N_3O_2P$
M_r	466.07	420.56	407.91	399.11	494.08	494.08
crystal system	monoclinic	monoclinic	monoclinic	monoclinic	tetragonal	tetragonal
space group	$P2_1/c$	$P2_1/c$	$P2_1/c$	$P2_1/a$	$P4_3$[c]	$P4_1$[c]
T [K]	293	293	293	293	223	223
a [Å]	8.501(1)	8.4895(4)	8.514(4)	8.951(5)	7.9357(7)	7.9389(7)
b [Å]	19.951(3)	18.888(7)	18.763(9)	13.049(7)	7.9357(7)	7.9389(7)
c [Å]	9.6221(2)	9.227(2)	9.071(4)	12.215(7)	28.283(3)	28.250(3)
α [°]	90	90	90	90	90	90
β [°]	108.4339(4)	105.094(2)	104.630(6)	94.210(9)	90	90
γ [°]	90	90	90	90	90	90
V [Å^3]	1548.2(2)	1428.5(6)	1402(1)	1422(1)	1781.1(3)	1780.5(3)
Z	4	4	4	4	4	4
ρ_{calcd} [g cm^{-1}]	1.999	1.955	1.932	1.863	1.842	1.843
μ ($Mo_{K\alpha}$) [mm^{-1}]	1.473	1.621	1.482	1.443	1.290	1.291
2θ range [°]	5.5–54.6	5.5–53.4	5.5–55.0	5.5–55.0	5.5–55.0	5.5–55.0
GOF on F^2	2.102	1.365	1.452	1.007	1.682	1.743
R_1[a] [$I>2\sigma(I)$]	0.053	0.039	0.044	0.033	0.073	0.080
wR_2[b] (all data)	0.155	0.132	0.119	0.088	0.165	0.161

[a] $R=\Sigma||F_o|-|F_c||/\Sigma|F_o|$. [b] $R_w=\{\Sigma w[(F_o^2-F_c^2)^2]/[(\Sigma wF_o^2)^2]\}^{1/2}$. [c] Space group is determined based on Flack parameters, which are 0.4(1) and −0.03(9) in **4a**⊃PF_6^-·MeOH and **4b**⊃PF_6^-·MeOH, respectively.

solution of $AgClO_4$·*n*H_2O (7.8 mg, 0.037 mmol) in water (1.5 mL), with a mixed solvent of ethanol/water (v/v 1:1, 1.5 mL) placed between the two layers (yield: 72%). FTIR: $\tilde{\nu}=3267$ (m; ν, N–H stretching band), 1656 (s; ν, amide-I), 1552 (s; δ, amide-II), 1088 cm^{-1} (s, multibands; ν, ClO_4^-); elemental analysis calcd (%) for $C_{12}H_{13}AgClN_3O_6$: C 32.86, H 2.99, N 9.58; found: C 32.76, H 2.81, N 9.65.

Synthesis of {[Ag(4-pmia)][NO_3]·H_2O}$_n$ (2⊃NO_3^-·H_2O): A solution of 4-pmia (16 mg, 0.075 mmol) in ethanol (1.5 mL) was gently layered on a solution of $AgNO_3$ (6.4 mg, 0.037 mmol) in water (1.5 mL), with a mixed solvent of ethanol/water (v/v 1:1, 1.5 mL) placed between the two layers (yield: 55%). FTIR: $\tilde{\nu}=3256$ (m; ν, N–H stretching band), 1655 (s; ν, amide-I), 1552 (s; δ, amide-II), 1385 cm^{-1} (s; ν, NO_3^-); elemental analysis calcd (%) for $C_{12}H_{13}AgN_4O_5$: C 35.93, H 3.27, N 13.97; found: C 36.34, H 3.02, N 14.28.

Synthesis of {[Ag(3-pmia)][PF_6]}$_n$ (3⊃PF_6^-): A solution of 3-pmia (32.0 mg, 0.150 mmol) in ethanol (1.5 mL) was carefully layered on a solution of $AgPF_6$ (19.0 mg, 0.075 mmol) in methanol/chloroform mixed solvent (v/v 9:1, 1.5 mL), with a mixed solvent of ethanol/chloroform (v/v 19:1, 1.5 mL) placed between the two layers (yield: 80%). FTIR: $\tilde{\nu}=$ 3295 (m; ν, N–H stretching band), 1660 (s; ν, amide-I), 1553 (s; δ, amide-II), 836 cm^{-1} (s, br; ν, PF_6^-); elemental analysis calcd (%) for $C_{12}H_{11}AgF_6N_3OP$: C 30.92, H 2.38, N 9.02; found: C 31.29, H 2.39, N 9.09.

Synthesis of {[Ag(3-pmia)][ClO_4]}$_n$ (3⊃ClO_4^-): A solution of 3-pmia (16.0 mg, 0.075 mmol) in ethanol (1.5 mL) was carefully layered on a solution of $AgClO_4$·*n*H_2O (7.77 mg, 0.038 mmol) in water (1.5 mL), with a mixed solvent of ethanol/water (v/v 1:1, 1.5 mL) placed between the two layers (yield: 72%). FTIR: $\tilde{\nu}=3285$ (m; ν, N–H stretching band), 1657 (s; ν, amide-I), 1552 (s; δ, amide-II), 1089 cm^{-1} (s, multibands; ν, ClO_4^-); elemental analysis calcd (%) for $C_{12}H_{11}AgClN_3O_5$: C 34.27, H 2.64, N 9.99; found: C 34.11, H 2.56, N 10.08.

Synthesis of {[Ag(3-pmia)][BF_4]}$_n$ (3⊃BF_4^-): A solution of 3-pmia (32.0 mg, 0.150 mmol) in ethanol (1.5 mL) was carefully layered on a solution of $AgBF_4$ (14.6 mg, 0.075 mmol) in methanol/chloroform mixed solvent (v/v 9:1, 1.5 mL), with a mixed solvent of ethanol/chloroform (v/v 19:1, 1.5 mL) placed between the two layers (yield: 27%). FTIR: $\tilde{\nu}=$ 3279 (m; ν, N–H stretching band), 1655 (s; ν, amide-I), 1555 (s; δ, amide-II), 1074 cm^{-1} (s, multibands; ν, BF_4^-); elemental analysis calcd (%) for $C_{12}H_{11}AgBF_4N_3O$: C 35.33, H 2.72, N 10.30; found: C 35.50, H 2.75, N 10.09.

Synthesis of {[Ag(3-pmia)][NO_3]·H_2O}$_n$ (3⊃NO_3^-·H_2O): A solution of 3-pmia (32 mg, 0.15 mmol) in ethanol (1.5 mL) was gently layered on a solution of $AgNO_3$ (13 mg, 0.075 mmol) in water (1.5 mL), with a mixed solvent of ethanol/water (v/v 1:1, 1.5 mL) placed between the layers (yield: 80%). FTIR: $\tilde{\nu}$ = 3259 (m; ν, N–H stretching band), 1657 (s; ν, amide-I), 1554 (s; δ, amide-II), 1384 cm^{-1} (s; ν, NO_3^-); elemental analysis calcd (%) for $C_{12}H_{13}AgN_4O_5$: C 35.93, H 3.27, N 13.97; found: C 35.66, H 3.20, N 14.08.

Synthesis of {[Ag(4-pmna)][PF_6]·MeOH}$_n$ (4⊃PF_6^-·MeOH): A solution of 4-pmna (16 mg, 0.075 mmol) in ethanol (1.5 mL) was carefully layered on a solution of $AgPF_6$ (9.5 mg, 0.038 mmol) in a methanol/chloroform mixed solvent (v/v 9:1, 1.5 mL), with a mixed solvent of ethanol/chloroform (v/v 19:1, 1.5 mL) placed between the two layers (yield: 60%). FTIR: $\tilde{\nu}$ = 3448 (m; ν, N–H stretching band), 1664 (s; ν, amide-I), 1533 (s; δ, amide-II), 841 cm^{-1} (s, br; ν, PF_6^-); elemental analysis calcd (%) for $C_{13}H_{15}AgF_6N_3O_2P$: C 31.35, H 3.04, N 8.44; found: C 31.87, H 3.01, N 8.63.

X-ray crystal analysis: All single crystals were mounted on a glass fiber and coated with epoxy resin. For each compound, X-ray data collections were carried out by using a Rigaku Mercury diffractometer with graphite-monochromated $Mo_{K\alpha}$ radiation (λ = 0.71069 Å) and a charge-coupled device (CCD) two-dimensional detector. Two different χ settings were used and ω were changed by 0.5° per frame. Intensity data were collected with a ω scan width of 0.5°. Empirical absorption correction using REQABA[25] was performed for all data. Crystal data and details of the structure determinations are summarized in Table 6. The structures of **1**⊃NO_3^-, **2**⊃PF_6^-, **3**⊃ClO_4^-, **3**⊃BF_4^-, and **3**⊃NO_3^-·H_2O were solved by a direct method using the SIR97 program[26] and expanded using Fourier techniques.[27] The structure of **2**⊃ClO_4^-·H_2O was solved by a direct method using the SIR92 program[28] and expanded using Fourier techniques.[27] The structure of **3**⊃PF_6^- was solved by a direct method using the SAPI91 program[29] and expanded using Fourier techniques.[27] The structures of **1**⊃PF_6^-, **1**⊃ClO_4^-, **1**⊃BF_4^-, **2**⊃NO_3^-·H_2O, **4a**⊃PF_6^-·MeOH, and **4b**⊃PF_6^-·MeOH were solved by a direct method using the DIRDIF (Patty) program[30] and expanded using Fourier techniques.[27] The final cycles of the full-matrix least-squares refinements were based on the observed reflections. All calculations were performed by using the teXsan crystallographic software package of Molecular Structure Corporation.[31] For all compounds the non-hydrogen atoms were refined anisotropically and all the hydrogen atoms were placed in the ideal positions. In **1**⊃ClO_4^-, the disorder of the perchlorate anion containing Cl(1) and O(2)–C(4) was found at a final stage, and thus its atom positions were isotropically refined under a rigid condition. In compound **2**⊃PF_6^-, the F(8) atom was refined isotropically. In **2**⊃ClO_4^-·H_2O, the water molecule of the O(6) atom was refined isotropically. In **2**⊃NO_3^-·H_2O, the water molecule of the O(5) atom was refined isotropically. In **3**⊃NO_3^-·H_2O, the water molecule of the O(5) atom was refined isotropically. In **4a**⊃PF_6^-·MeOH, the F(2)–F(3), O(2), and C(13) atoms were refined isotropically. In **4b**⊃PF_6^-·MeOH, the F(3)–F(4), O(2), and C(13) atoms were refined isotropically. CCDC-686311 (**1**⊃PF_6^-), 686312 (**1**⊃ClO_4^-), 686313 (**1**⊃BF_4^-), 686314 (**1**⊃NO_3^-), 686315 (**2**⊃PF_6^-), 686316 (**2**⊃ClO_4^-·H_2O), 686317 (**2**⊃NO_3^-·H_2O), 686318 (**3**⊃PF_6^-), 686319 (**3**⊃ClO_4^-), 686320 (**3**⊃BF_4^-), 686321 (**3**⊃NO_3^-·H_2O), 686322 (**4a**⊃PF_6^-·MeOH), and 686323 (**4b**⊃PF_6^-·MeOH) contain the supplementary crystallographic data for this paper. These data can be obtained free of charge from the Cambridge Crystallographic Data Centre via www.ccdc.cam.ac.uk/data_request/cif. The microcrystalline samples of **1**–**3** were prepared in the same solvent, and the crystallinity was checked by X-ray powder diffraction (XRPD) as shown in Figures S6–S8 (see the Supporting Information).

Physical measurements: Infrared (IR) spectra were recorded on a Perkin-Elmer 2000 FTIR spectrophotometer with samples prepared as a Nujol mull. XRPD data were collected on a Rigaku RINT-2200 (Ultima) diffractometer using $Cu_{K\alpha}$ radiation.

Acknowledgement

This work was supported by the Grants-in-Aid for Scientific Research (Young Scientist (B) No. 19750048).

[1] a) M. J. Zaworotko, *Chem. Soc. Rev.* **1994**, *23*, 283–288; b) S. R. Batten, R. Robson, *Angew. Chem.* **1998**, *110*, 1558–1595; *Angew. Chem. Int. Ed.* **1998**, *37*, 1460–1494; c) B. Moulton, M. J. Zaworotko, *Chem. Rev.* **2001**, *101*, 1629–1658; d) O. M. Yaghi, M. O'Keeffe, N. W. Ockwig, H. K. Chae, M. Eddaoudi, J. Kim, *Nature* **2003**, *423*, 705–714; e) S. Kitagawa, R. Kitaura, S.-i. Noro, *Angew. Chem.* **2004**, *116*, 2388–2430; *Angew. Chem. Int. Ed.* **2004**, *43*, 2334–2375.

[2] For reviews of supramolecular assembles in the solid state, see: a) A. D. Burrows, C.-W. Chan, M. M. Chowdhry, J. E. McGrady, D. M. P. Mingos, *Chem. Soc. Rev.* **1995**, *24*, 329–339; b) J. Bernstein, R. E. Davis, L. Shimoni, N.-L. Chang, *Angew. Chem.* **1995**, *107*, 1689–1708; *Angew. Chem. Int. Ed. Engl.* **1995**, *34*, 1555–1573; c) G. R. Desiraju, *Angew. Chem.* **1995**, *107*, 2541–2558; *Angew. Chem. Int. Ed. Engl.* **1995**, *34*, 2311–2327; d) R. Bishop, *Chem. Soc. Rev.* **1996**, *25*, 311–319; e) C. B. Aakeröy, A. M. Beatty, *Aust. J. Chem.* **2001**, *54*, 409–421; f) D. T. Bong, T. D. Clark, J. R. Granja, M. R. Ghadiri, *Angew. Chem.* **2001**, *113*, 1016–1041; *Angew. Chem. Int. Ed.* **2001**, *40*, 988–1011; g) L. R. Nassimbeni, *Acc. Chem. Res.* **2003**, *36*, 631–637; h) I. G. Georgiev, L. R. MacGillivray, *Chem. Soc. Rev.* **2007**, *36*, 1239–1248.

[3] For examples of supramolecular assembles in the solid state, see: a) X. Zhao, Y.-L. Chang, F. W. Fowler, J. W. Lauher, *J. Am. Chem. Soc.* **1990**, *112*, 6627–6634; b) M. C. Etter, Z. Urbakzyk-Lipkowska, M. Zia-Ebrahimi, T. W. Panunto, *J. Am. Chem. Soc.* **1990**, *112*, 8415–8426; c) M. Simard, D. Su, J. D. Wuest, *J. Am. Chem. Soc.* **1991**, *113*, 4696–4698; d) F. Garcia-Tellado, S. J. Geib, S. Goswami, A. D. Hamilton, *J. Am. Chem. Soc.* **1991**, *113*, 9265–9269; e) D. Venkataraman, S. Lee, J. Zhang, J. S. Moore, *Nature* **1994**, *371*, 591–593; f) X. Wang, M. Simard, J. D. Wuest, *J. Am. Chem. Soc.* **1994**, *116*, 12119–12120; g) A. T. Ung, D. Gizachew, R. Bishop, M. L. Scudder, I. G. Dance, D. C. Craig, *J. Am. Chem. Soc.* **1995**, *117*, 8745–8756; h) L. R. MacGillivray, J. L. Atwood, *Nature* **1997**, *389*, 469–472; i) T. Sawaki, Y. Aoyama, *J. Am. Chem. Soc.* **1999**, *121*, 4793–4798; j) K. T. Holman, A. M. Pivovar, M. D. Ward, *Science* **2001**, *294*, 1907–1911; k) T. L. Nguyen, F. W. Fowler, J. W. Lauher, *J. Am. Chem. Soc.* **2001**, *123*, 11057–11064; l) C. B. Aakeröy, A. M. Beatty, B. A. Helfrich, *J. Am. Chem. Soc.* **2002**, *124*, 14425–14432; m) K. Kobayashi, A. Sato, S. Sakamoto, K. Yamaguchi, *J. Am. Chem. Soc.* **2003**, *125*, 3035–3045; n) K. Sada, K. Inoue, T. Tanaka, A. Tanaka, A. Epergyes, S. Nagahama, A. Matsumoto, M. Miyata, *J. Am. Chem. Soc.* **2004**, *126*, 1764–1771.

[4] S. Kitagawa, K. Uemura, *Chem. Soc. Rev.* **2005**, *34*, 109–119.

[5] Mononuclear complex assembles with py-amide ligands: a) C. B. Aakeröy, A. M. Beatty, D. S. Leinen, *J. Am. Chem. Soc.* **1998**, *120*, 7383–7384; b) C. B. Aakeröy, A. M. Beatty, *Chem. Commun.* **1998**, 1067–1068; c) C. B. Aakeröy, A. M. Beatty, B. A. Helfrich, *J. Chem. Soc. Dalton Trans.* **1998**, 1943–1945; d) J. C. Noveron, M. S. Lah, R. E. D. Sesto, A. M. Arif, J. S. Miller, P. J. Stang, *J. Am. Chem. Soc.* **2002**, *124*, 6613–6625.

[6] Coordination polymers including py-urea-py-type ligands: a) C. L. Schauer, E. Matwey, F. W. Fowler, J. W. Lauher, *J. Am. Chem. Soc.* **1997**, *119*, 10245–10246; b) D. K. Kumar, D. A. Jose, A. Das, P. Dastidar, *Inorg. Chem.* **2005**, *44*, 6933–6935; c) R. Custelcean, B. A. Moyer, V. S. Bryantsev, B. P. Hay, *Cryst. Growth Des.* **2006**, *6*, 555–563; d) D. K. Kumar, A. Das, P. Dastidar, *New J. Chem.* **2006**, *30*, 1267–1274.

[7] Coordination polymers including unsymmetrical py-amide-py-type ligands: a) M. Kondo, A. Asami, H.-C. Chang, S. Kitagawa, *Cryst. Eng.* **1999**, *2*, 115–122; b) Z. Qin, M. C. Jennings, R. J. Puddephatt, *Chem. Commun.* **2001**, 2676–2677; c) Z. Qin, M. C. Jennings, R. J. Puddephatt, *Chem. Commun.* **2002**, 354–355; d) M.-L. Tong, Y.-M. Wu, J. Ru, X.-M. Chen, H.-C. Chang, S. Kitagawa, *Inorg. Chem.* **2002**, *41*, 4846–4848; e) D. K. Kumar, A. Das, P. Dastidar, *Cryst.*

Growth Des. **2006**, *6*, 1903–1909; f) D. K. Kumar, A. Das, P. Dastidar, *J. Mol. Struct.* **2006**, *796*, 139–145.

[8] a) K. Uemura, S. Kitagawa, M. Kondo, K. Fukui, R. Kitaura, H.-C. Chang, T. Mizutani, *Chem. Eur. J.* **2002**, *8*, 3586–3600; b) K. Uemura, S. Kitagawa, K. Fukui, K. Saito, *J. Am. Chem. Soc.* **2004**, *126*, 3817–3828; c) K. Uemura, K. Saito, S. Kitagawa, H. Kita, *J. Am. Chem. Soc.* **2006**, *128*, 16122–16130.

[9] Coordination polymers including symmetrical py-(amide)$_2$-py-type ligands: a) S. Muthu, J. H. K. Yip, J. J. Vittal, *J. Chem. Soc. Dalton Trans.* **2001**, 3577–3584; b) S. Muthu, J. H. K. Yip, J. J. Vittal, *J. Chem. Soc. Dalton Trans.* **2002**, 4561–4568; c) T. J. Burchell, D. J. Eisler, M. C. Jennings, R. J. Puddephatt, *Chem. Commun.* **2003**, 2228–2229; d) C.-H. Ge, X.-D. Zhang, P. Zhang, W. Guan, F. Guo, Q.-T. Liu, *Polyhedron* **2003**, *22*, 3493–3497; e) T. J. Burchell, D. J. Eisler, R. J. Puddephatt, *Chem. Commun.* **2004**, 944–945; f) M. Sarkar, K. Biradha, *Chem. Commun.* **2005**, 2229–2231; g) M. Sarkar, K. Biradha, *Cryst. Growth Des.* **2006**, *6*, 1742–1745; h) M. Sarkar, K. Biradha, *Eur. J. Inorg. Chem.* **2006**, 531–534; i) M. Sarkar, K. Biradha, *Cryst. Growth Des.* **2007**, *7*, 1318–1331.

[10] C. Branden, J. Tooze, *Introduction to Protein Structure*, 2nd ed., Garland, New York, **1999**.

[11] F. A. Cotton, G. Wilkinson, *Advanced Inorganic Chemistry*, 5th ed., Wiley, Chichester, **1988**.

[12] a) M. Munakata, L. P. Wu, G. L. Ning, *Coord. Chem. Rev.* **2000**, *198*, 171–203; b) A. N. Khlobystov, A. J. Blake, N. R. Champness, D. A. Lemenovskii, A. G. Majouga, N. V. Zyk, M. Schroder, *Coord. Chem. Rev.* **2001**, *222*, 155–192; c) C.-L. Chen, B.-S. Kang, C.-Y. Su, *Aust. J. Chem.* **2006**, *59*, 3–18.

[13] For examples of linear Ag^I coordination polymers, see: a) R. G. Vranka, E. L. Amma, *Inorg. Chem.* **1966**, *5*, 1020–1025; b) L. Carlucci, G. Ciani, D. M. Proserpio, A. Sironi, *J. Am. Chem. Soc.* **1995**, *117*, 4562–4569; c) F. Robinson, M. J. Zawarotko, *J. Chem. Soc. Chem. Commun.* **1995**, 2413–2414; d) O. M. Yaghi, H. Li, *J. Am. Chem. Soc.* **1996**, *118*, 295–296; e) M. A. Withersby, A. J. Blake, N. R. Champness, P. Hubberstey, W.-S. Li, M. Schroder, *Angew. Chem.* **1997**, *109*, 2421–2423; *Angew. Chem. Int. Ed. Engl.* **1997**, *36*, 2327–2329; f) A. J. Blake, N. R. Champness, A. N. Khlobystov, D. A. Lemenovskii, W.-S. Lia, M. Schroder, *Chem. Commun.* **1997**, 1339–1340; g) A. J. Blake, G. Baum, N. R. Champness, S. S. M. Chung, P. A. Cooke, D. Fenske, A. N. Khlobystov, D. A. Lemenovskii, W.-S. Li, M. Schroder, *J. Chem. Soc. Dalton Trans.* **2000**, 4285–4291; h) R. Horikoshi, T. Mochida, N. Maki, S. Yamada, H. Moriyama, *J. Chem. Soc. Dalton Trans.* **2002**, 28–33.

[14] D. M. P. Mingos, A. L. Rohl, *Inorg. Chem.* **1991**, *30*, 3769–3771.

[15] a) J.-M. Lehn, A. Rigault, J. Siegel, J. Harrowfield, B. Chevrier, D. Moras, *Proc. Natl. Acad. Sci. USA* **1987**, *84*, 2565–2569; b) E. C. Constable, *Tetrahedron* **1992**, *48*, 10013–10059; c) C. Piguet, G. Bernardinelli, G. Hopfgartner, *Chem. Rev.* **1997**, *97*, 2005–2062.

[16] a) C. Piguet, G. Bernardinelli, B. Bocquet, A. Quattropani, A. F. Williams, *J. Am. Chem. Soc.* **1992**, *114*, 7440–7451; b) R. F. Carina, G. Bernardinelli, A. F. Williams, *Angew. Chem.* **1993**, *105*, 1483–1485; *Angew. Chem. Int. Ed. Engl.* **1993**, *32*, 1463–1465; c) D. M. L. Goodgame, S. P. W. Hill, D. J. Williams, *J. Chem. Soc. Chem. Commun.* **1993**, 1019–1021; d) N. Ohata, H. Masuda, O. Yamauchi, *Angew. Chem.* **1996**, *108*, 570–572; *Angew. Chem. Int. Ed. Engl.* **1996**, *35*, 531–532; e) L. Carlucci, G. Ciani, D. W. v. Gudenberg, D. M. Proserpio, *Inorg. Chem.* **1997**, *36*, 3812–3813; f) M. Albrecht, *Chem. Rev.* **2001**, *101*, 3457–3497; g) X.-L. Wang, C. Qin, E.-B. Wang, L. Xu, Z.-M. Su, C.-W. Hu, *Angew. Chem.* **2004**, *116*, 5146–5150; *Angew. Chem. Int. Ed.* **2004**, *43*, 5036–5040.

[17] The plots of *b* versus *a* are shown in Figure S9 in the Supporting Information.

[18] M. Sarkar, K. Biradha, *Cryst. Growth Des.* **2006**, *6*, 202–208.

[19] A single chain and neighboring chains of **2**⊃PF_6^- take the form -A-A-A-A- to afford a two-dimensional sheet of ligands with the same conformation. In contrast, neighboring two-dimensional sheets consist of -B-B-B-B- chains.

[20] a) J. L. Atwood, K. T. Holman, J. W. Steed, *Chem. Commun.* **1996**, 1401–1407; b) B. H. M. Snellink-Ruel, M. M. G. Antonisse, J. F. J. Engbersen, P. Timmerman, D. N. Reinhoudt, *Eur. J. Org. Chem.* **2000**, 165–170; c) P. D. Beer, P. A. Gale, *Angew. Chem.* **2001**, *113*, 502–532; *Angew. Chem. Int. Ed.* **2001**, *40*, 486–516; d) R. Vilar, *Angew. Chem.* **2003**, *115*, 1498–1516; *Angew. Chem. Int. Ed.* **2003**, *42*, 1460–1477; e) C. R. Bondy, S. J. Loeb, *Coord. Chem. Rev.* **2003**, *240*, 77–99; f) J. L. Atwood, A. Szumna, *Chem. Commun.* **2003**, 940–941; g) K. Bowman-James, *Acc. Chem. Res.* **2005**, *38*, 671–678; h) B. P. Hay, T. K. Firman, B. A. Moyer, *J. Am. Chem. Soc.* **2005**, *127*, 1810–1819; i) R. Custelcean, M. G. Gorbunova, *J. Am. Chem. Soc.* **2005**, *127*, 16362–16363; j) N. Gimeno, R. Vilar, *Coord. Chem. Rev.* **2006**, *250*, 3161–3189; k) M. H. Filby, J. W. Steed, *Coord. Chem. Rev.* **2006**, *250*, 3200–3218.

[21] a) B. F. Hoskins, R. Robson, *J. Am. Chem. Soc.* **1990**, *112*, 1546–1554; b) K. S. Min, M. P. Suh, *J. Am. Chem. Soc.* **2000**, *122*, 6834–6840; c) O.-S. Jung, Y. J. Kim, Y.-A. Lee, J. K. Park, H. K. Chae, *J. Am. Chem. Soc.* **2000**, *122*, 9921–9925; d) O.-S. Jung, Y. J. Kim, Y.-A. Lee, H. K. Chae, H. G. Jang, J. Hong, *Inorg. Chem.* **2001**, *40*, 2105–2110; e) E. Lee, J. Kim, J. Heo, D. Whang, K. Kim, *Angew. Chem.* **2001**, *113*, 413–416; *Angew. Chem. Int. Ed.* **2001**, *40*, 399–402; f) B. Sui, J. Fan, T.-a. Okamura, W.-Y. Sun, N. Ueyama, *New J. Chem.* **2001**, *25*, 1379–1381; g) S.-i. Noro, R. Kitaura, M. Kondo, S. Kitagawa, T. Ishii, H. Matsuzaka, M. Yamashita, *J. Am. Chem. Soc.* **2002**, *124*, 2568–2583; h) S. A. Dalrymple, G. K. H. Shimizu, *Chem. Eur. J.* **2002**, *8*, 3010–3015; i) A. N. Khlobystov, N. R. Champness, C. J. Roberts, S. J. B. Tendler, C. Thompson, M. Schroder, *CrystEngComm* **2002**, *4*, 426–431; j) J. Fan, L. Gan, H. Kawaguchi, W.-Y. Sun, K.-B. Yu, W.-X. Tang, *Chem. Eur. J.* **2003**, *9*, 3965–3973; k) D. R. Turner, E. C. Spencer, J. A. K. Howard, D. A. Tocher, J. W. Steed, *Chem. Commun.* **2004**, 1352–1353.

[22] The results are shown in Figures S10 and S11 in the Supporting Information.

[23] Schematic views of the anion environments in **1**⊃X are shown in Figure S1 in the Supporting Information.

[24] Although **3**⊃BF_4^- forms similar structural motifs to **3**⊃PF_6^- and **3**⊃ClO_4^-, anion exchange proceeds readily. This is probably because of the different crystal-packing force attributed to BF_4^- (38 Å^3), which is much smaller than that of PF_6^- (54 Å^3) and ClO_4^- (47 Å^3).

[25] R. A. Jacobson, REQABA Empirical Absorption Correction, The Woodlands, TX (USA), **1996–1998**.

[26] A. Altomare, M. C. Burla, M. Camalli, G. L. Cascarano, C. Giacovazzo, A. Guagliardi, A. G. G. Moliterni, G. Polidori, R. Spagna, *J. Appl. Crystallogr.* **1999**, *32*, 115–119.

[27] P. T. Beurskens, G. Admiraal, G. Beurskens, W. P. Bosman, R. de-Gelder, R. Israel, J. M. M. Smits, The DIRDIF-94 Program System, Technical Report of the Crystallography Laboratory, University of Nijmegen (The Netherlands), **1994**.

[28] A. Altomare, M. C. Burla, M. Camalli, M. Cascarano, C. Giacovazzo, A. Guagliardi, G. Polidori, *J. Appl. Crystallogr.* **1994**, *27*, 435.

[29] F. Hai-Fu, Structure Analysis Programs with Intelligent Control, Rigaku Corporation, Tokyo (Japan), **1991**.

[30] P. T. Beurskens, G. Admiraal, G. Beurskens, W. P. Bosman, S. Garcia-Granda, R. O. Gould, J. M. M. Smits, C. Smykalla, The DIRDIF Program System, Technical Report of the Crystallography Laboratory, University of Nijmegen (The Netherlands), **1992**.

[31] teXsan Crystal Structure Analysis Package, Molecular Structure Corporation, The Woodlands, TX (USA), **2000**.

Received: April 28, 2008
Published online: September 9, 2008

